ResearchGate

See discussions, stats, and author profiles for this publication at: https://www.researchgate.net/publication/215462398

Perylenediimide-Linked DNA Dumbbells: Long-Distance Electronic Interactions and Hydrophobic Assistance of Base-Pair Melting†

ARTICLE *in* THE JOURNAL OF PHYSICAL CHEMISTRY C · DECEMBER 2010

Impact Factor: 4.77 · DOI: 10.1021/jp1048309

CITATIONS
10

READS
23

6 AUTHORS, INCLUDING:

Mahesh Hariharan
Indian Institute Of Science Education and …
45 PUBLICATIONS **843** CITATIONS
SEE PROFILE

Karsten Siegmund
Northwestern University
16 PUBLICATIONS **192** CITATIONS
SEE PROFILE

Hai Long
National Renewable Energy Laboratory
37 PUBLICATIONS **778** CITATIONS
SEE PROFILE

Frederick D Lewis
Northwestern University
319 PUBLICATIONS **9,207** CITATIONS
SEE PROFILE

Available from: Mahesh Hariharan
Retrieved on: 26 January 2016

Perylenediimide-Linked DNA Dumbbells: Long-Distance Electronic Interactions and Hydrophobic Assistance of Base-Pair Melting†

Mahesh Hariharan,‡ Karsten Siegmund, Yan Zheng,§ Hai Long,|| George C. Schatz, and Frederick D. Lewis*

Department of Chemistry, Northwestern University, Evanston, Illinois 60208-3113

Received: May 26, 2010; Revised Manuscript Received: July 20, 2010

The synthesis and properties of synthetic DNA dumbbells having A-tract base pair domains consisting of 6−16 base pairs connected by perylenediimide (PDI) linkers are reported. The dumbbells were prepared in good yield by chemical ligation of nicked-dumbbell precursors having six or more A-T base pairs. The dumbbell structures have been investigated by a combination of electronic spectroscopy and molecular dynamics simulations. UV−visible spectra are indicative of the formation of monomeric dumbbells at room temperature in aqueous buffer in the absence of added salt. The long-wavelength region of the circular dichroism (CD) spectra is a composite of induced CD of the PDI monomers and intramolecular exciton-coupled CD between the two PDI chromophores. Weak exciton coupled CD can be observed between PDI chromophores separated by 13 base pairs, thus extending the reach of dumbbell molecular rulers. Upon heating, the dumbbells undergo base pair melting and intramolecular PDI−PDI association. Analysis of the temperature-dependent spectral data provides evidence for a three-state model in which base pair melting of the intact dumbbell results in the formation of an intermediate species which is in equilibrium with a collapsed dumbbell having intramolecular PDI−PDI stacking. The low melting temperatures of the shorter dumbbells are attributed to the partial compensation of PDI−PDI association for base pair dissociation.

Introduction

The formation of synthetic DNA dumbbells having non-natural linkers connecting base-paired domains has been reported for a number of linkers including saturated alkanes,[1] oligo(ethylene glycol)s,[2] and aromatic dicarboxamides.[3−5] Dumbbells possessing dodecyl chains as linkers are reported to be more stable than corresponding dumbbells having T_4 loops by ca. 2 kcal/mol, a difference which is largely entropic in origin.[1] The melting of alkane-linked dumbbells at low salt concentrations can be analyzed using a simple two-state model in which the base pairs are either intact or fully dissociated. The melting of dumbbells having oligo(ethylene glycol) and stilbenedicarboxamide linkers is also consistent with a two-state model.[2,5] Dumbbells possessing short base pair domains are significantly more stable than the corresponding hairpins which possess a single linker or the nicked-dumbbell precursors of the intact dumbbells.[2,3,5]

We have employed synthetic dumbbell and nicked-dumbbell conjugates possessing arenedicarboxamide chromophores separated by A-tract base pair domains of varying length to investigate the distance and angle dependence of exciton-coupled circular dichroism (EC-CD)[5−7] and fluorescence resonance energy transfer (FRET).[8,9] The base pair domain functions as a helical ruler in these experiments, determining both the distance and angle between the electronic transition dipole moments of the two chromophores. The use of identical stilbenedicarboxamide chromophores enabled the observation of EC-CD over distances as large as 41 Å (11 intervening A-T base pairs).[7] The use of a stilbenedicarboxamide fluorescence donor and perylenediimide fluorescence acceptor permitted confirmation of the dependence of FRET intensity on the relative orientation of the transition dipoles, thus providing experimental verification of the orientation dependence originally proposed by Förster.[8,10]

Our interest in electronic interactions between oriented transition dipoles led us to investigate the structure and properties of DNA dumbbells possessing perylenediimide (PDI) linkers. PDI linkers offer the attractive feature of strong, structured absorption and fluorescence in the visible region for studies and applications involving energy transfer or electron transfer. PDI-linked bis(oligonucleotide) conjugates have been reported to form a variety of single strand[11] and base-paired structures, including duplexes,[12−14] triplexes,[15] hairpins,[16] and capped hairpins,.[17] Both duplex formation between complementary conjugates[13,14] and hydrophobic association of PDI-linked hairpins[16] have been observed to result in changes in the UV and fluorescence spectra characteristic of PDI dimer formation.

We report here the preparation and characterization of a series of PDI-linked DNA dumbbells (Chart 1). These dumbbells exist predominantly as monomers in dilute aqueous solution in the absence of added salt, thus permitting the investigation of both the electronic interactions between PDI separated by a variable number of A-T base pairs and assistance of base pair melting by intramolecular PDI-PDI association in the melted dumbbells. The monomer dumbbells undergo salt- and concentration-dependent aggregation, a process that will be described separately.

Results

Preparation of the Dumbbell Conjugates. The dumbbell precursors **P*n*** (n = 6−10, 13, and 16; Scheme 1) were

† Part of the "Mark A. Ratner Festschrift".

* To whom correspondence should be addressed. E-mail: fdl@northwestern.edu.

‡ Present address: School of Chemistry, Indian Institute of Science Education and Research Thiruvananthapuram, India.

§ Present address: PolyEra Corporation, Skokie, IL 60077.

|| Present address: National Renewable Energy Laboratory, Computational Materials Science Center, Golden, CO 80401.

10.1021/jp1048309 © 2010 American Chemical Society
Published on Web 08/04/2010

CHART 1: Structures for the Perylenediimide (PDI) Linker L and Base-Paired Dumbbells D6−D10, D13, and D16 and Hairpin H8

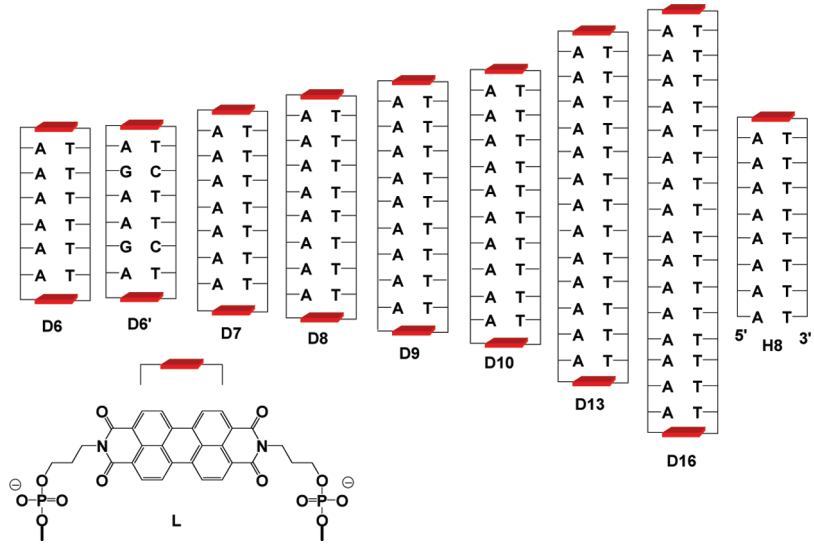

SCHEME 1: Chemical Ligation of Nicked Dumbbells P*l*,*m* Yields the Corresponding Dumbbells D*n* Possessing the Same Number of Intervening A-T Base Pairs

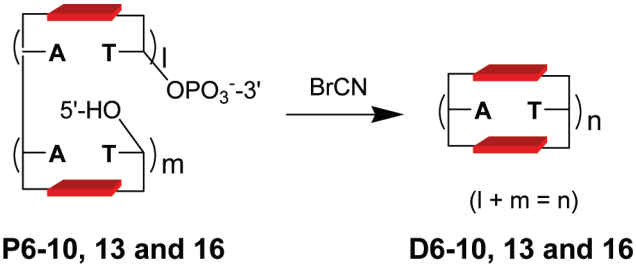

synthesized on a 3′-phosphate solid support following the procedure of Letsinger and Wu for the synthesis of bis(oligonucleotide) conjugates,[18] as modified by Rahe et al. for the incorporation of the PDI linker **L**.[17] Following cleavage, deprotection, and purification procedures, the 3′-phosphorylated sequences were annealed in 250 mM MES buffer at pH 7.6 in the presence of 20 mM $MgCl_2$ and reacted with CNBr,[19] providing the corresponding dumbbells **D*n***.[5] The dumbbells were purified using RP-HPLC (Figure S1, Supporting Information) and characterized using MALDI-TOF ms (Table S1, Supporting Information). The yields of the ligated dumbbells are dependent upon the length of the A-tract sequences, increasing from 70% for **D6** to >95% for **D16**. No ligation was observed for a nicked dumbbell precursor having two A-T base pairs on either side of the nick (Scheme 1, $l = m = 2$).

Absorption Spectra. The UV−vis absorption spectra of conjugates **D13** and **D8** at several temperatures are shown in Figure 1 and Figure S2 (Supporting Information), respectively. The long-wavelength band (>400 nm) is assigned to the PDI chromophores, whereas the short-wavelength band is assigned to overlapping absorption of PDI and the nucleobases. The appearance of the long wavelength bands of **D13** and the other conjugates having nine or more A-T base pairs is similar to that of the monomer hairpin **H8** (Chart 1) and has an A^{0-0}/A^{0-1} band intensity ratio of ca. 1.5:1, characteristic of monomeric PDI derivatives including **H8**.[16] Somewhat lower A^{0-0}/A^{0-1} band intensity ratios are observed for conjugates possessing eight or fewer A-T base pairs. Maximum band intensity ratios are summarized in Table 1. The band intensity ratio for **D13** is independent of concentration (0.5−2.0 μM) and temperature

TABLE 1: Maximum Values of the A^{0-0}/A^{0-1} Band Intensity Ratio and Melting Temperature for 2 μM Dumbbell in 10 mM Phosphate Buffer Obtained from the 260 nm Absorption Spectral Data (T_{260}) and A^{0-0}/A^{0-1} Ratios (T_{ratio})

conjugate	A^{0-0}/A^{0-1} [a]	T_{260}, °C[b]	T_{ratio}, °C[c]
D6	1.2	42.2	44.1
D7	1.3	49.5	50.7
D8	1.3	55.0	56.2
D9	1.6	69.3	70.1
D10	1.6	71.8	72.1
D13	1.5	79.3	78.2
D16	1.5	80.7	80.3
H8	1.5	39.3	

[a] Maximum value of the A^{0-0}/A^{0-1} band intensity ratio (estimated error ±0.1). [b] Data obtained by fitting the 260 nm melting profiles using Meltwin.[20] [c] Data obtained by fitting the A^{0-0}/A^{0-1} band intensity ratio using Meltwin.[20]

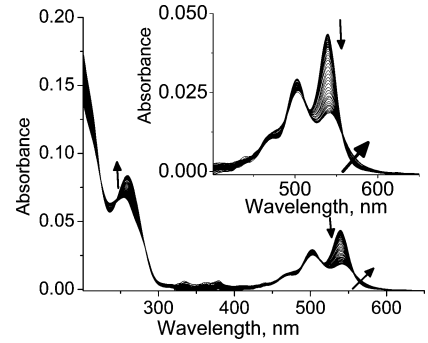

Figure 1. Temperature dependent absorption spectra of conjugate **D13** (1 μM) in 10 mM phosphate buffer (pH 7.2). Arrows indicate changes which occur upon heating from 5 to 95 °C in 1 °C steps.

(0−25 °C); however, the ratio for **D6** decreases with increasing concentration and decreasing temperature, indicative of partial aggregation in 10 mM sodium phosphate buffer similar to that observed for **H8**.

As seen in Figure 1, the 260 nm absorbance of **D13** increases with increasing temperature, whereas the A^{0-0}/A^{0-1} band intensity ratio decreases. Thermal dissociation profiles for **D8** and **D13** are shown in Figure 2. Both the 260 nm thermal dissociation profiles and the A^{0-0}/A^{0-1} band intensity ratios

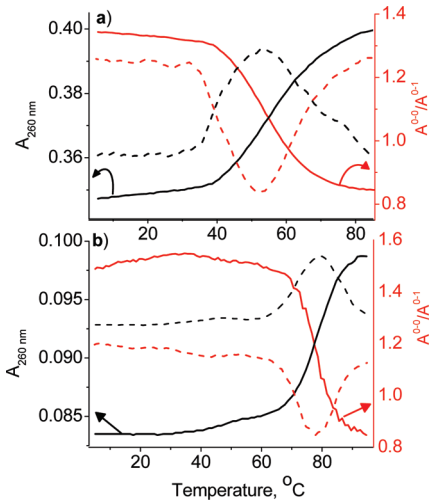

Figure 2. Thermal profiles for (a) **D8** and (b) **D13** in 10 mM phosphate buffer (pH 7.2) monitored at 260 nm (black lines, left axis) and the ratio A^{0-0}/A^{0-1} (red lines, right axis). Dashed lines represent corresponding differential curves.

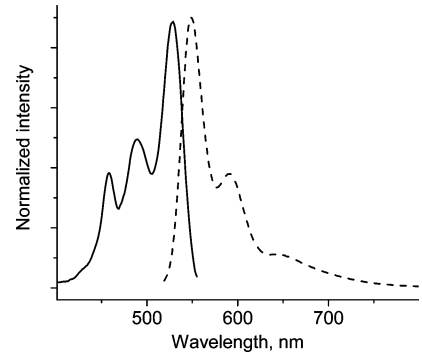

Figure 3. Fluorescence excitation spectrum (solid line, $\lambda_{em} = 570$ nm) and emission spectrum (dashed line, $\lambda_{ex} = 490$ nm) of dumbbell **D8** (1 μM, in 10 mM phosphate buffer, pH 7.2).

display a single melting transition above room temperature. Fitting of the thermal dissociation profiles using Meltwin[20] provides the values of T_{260} and T_{ratio} reported in Table 1. Similar values are obtained from the first derivatives of these plots, as shown in Figure 2 for **D8** and **D13**.

Fluorescence Spectra. The fluorescence excitation and emission spectra of **D8** at 25 °C in buffer are shown in Figure 3. Similar spectra are observed for the other conjugates. The fluorescence excitation spectra display vibronic band maxima and relative intensities similar to those of the absorption spectra (Figure 1). The fluorescence emission spectra have a mirror image relationship to the absorption and fluorescence excitation spectra with vibronic bands at 549, 591, and 655 nm. The fluorescence quantum yield of conjugate **D8** in buffer at 20 °C is 0.0091 ± 0.002. Upon heating, the fluorescence spectra of **D8** undergoes an initial decrease in intensity followed by and increase in intensity accompanied by a blue-shift in the vibronic bands but no increase in the intensity in the long-wavelength region (Figure S3, Supporting Information). The inflection point in a plot of the intensity of the short wavelength vibronic band versus temperature occurs at ca. 55 °C, similar to the values of T_m reported in Table 1.

Circular Dichroism Spectra. The CD spectra of the PDI dumbbells **D6, D8**, and **D13** in buffer are shown in Figure 4 along with the spectrum of the PDI-linked monomer hairpin **H8** (Chart 1) shown in the inset.[16] The short wavelength region of the CD spectra in buffer display positive bands at 280 nm

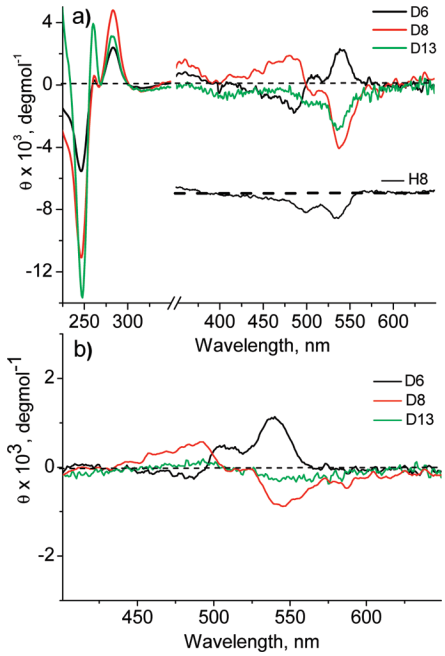

Figure 4. (a) Circular dichroism spectra of PDI dumbbell conjugates **D6**, **D8**, and **D13** and hairpin **H8** in 10 mM phosphate buffer (pH 7.2). (b) Spectra corrected for induced circular dichroism by subtraction of the spectrum of **H8** from the spectra of the dumbbells.

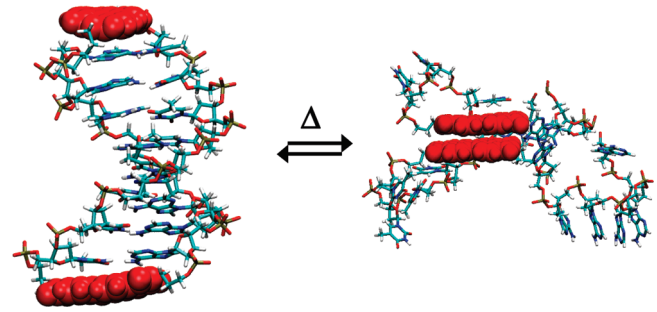

Figure 5. Molecular dynamics simulated structure of dumbbell **D8** before and after base pair melting.

and negative bands at 246 nm characteristic of relatively short poly(dA)−poly(dT) duplexes and hairpins.[7] In addition, the spectrum of **D13** displays a sharp positive band at 260 nm, characteristic of longer poly(dA)−poly(dT) duplexes and hairpins.[21] The long-wavelength portion of the CD spectra of dumbbell **D6** in buffer displays a positive/negative pattern (positive Cotton effect) attributed to exciton coupling between the PDI chromophores.[22] The long-wavelength spectra of **D8** and **D13** are similar to that of **D6** but with inverted signs (negative Cotton effect) and decreased intensity.

Molecular Modeling of the Monomer Dumbbell. Minimized structures for the monomeric base-paired dumbbells **D6**−**D10** were calculated using the AMBER force field and methods previously developed for stilbenedicarboxamide- and PDI-linked hairpins and dumbbells.[7,13] The calculated structure for **D8** is shown in Figure 5. All of the dumbbells have an average π-stacking distance of 3.3 ± 0.1 Å and a helical pitch of 31 ± 1.5°. These values are somewhat smaller than the average values for B-DNA (3.4 Å and 36°).[23] The minimized structure of the melted dumbbell **D8** shown in Figure 5 displays formation of an intramolecular PDI−PDI dimer connected by disordered poly(dA) and poly(dT) base sequences in such a way that nucleobases partially shield the external hydrophobic faces

of the PDI dimer. The dihedral angle between the PDI long axes in the melted structures is ca. 21°.

Discussion

Structure and Spectroscopy of Monomer Dumbbells. The synthesis of dumbbell conjugates possessing PDI linkers employed chemical ligation of nicked dumbbell precursors (Scheme 1), as previously implemented for synthesis of dumbbell conjugates possessing stilbenedicarboxamide and PEG linkers.[2,5] The attempted ligation of a nicked dumbbell possessing two A-T base pairs on either side of the nick was unsuccessful and led only to the recovered nicked dumbbell. Ligation requires close proximity of the dT bases on either side of the nick.[19] We suspect that unsuccessful ligation of the shorter nicked dumbbell is a consequence of intermolecular PDI−PDI hydrophobic association (vide infra) which overpowers A-T base pairing. No such difficulties were encountered in the ligation of short nicked dumbbells having stilbenedicarboxamide or PEG linkers.[2,5] Incorporation of stronger G-C base pairs might facilitate the synthesis of shorter PDI-linked dumbbells.

The structure of the PDI-linked dumbbell **D8** in water obtained from a molecular dynamics simulation (Figure 5) is similar to that previously reported for the corresponding stilbenedicarboxamide-linked dumbbells.[5] These structures have B-DNA base-pair domains linked by chromophores which are π-stacked with the adjacent base pairs. Support for the formation of a base-paired structure in which the PDI chromophores are separated by a poly(dA)−poly(dT) base pair domain is provided by their electronic spectra. The 260 nm absorption bands of the dumbbells are dominated by the base pairs and display a single melting transition with ca. 25% hypochromism (Figure 1 and Supporting Information Figure S2), as expected for A-tract base pair melting (Figure 2a).[18] The short wavelength region of the CD spectra (Figure 3) also displays a structure characteristic of poly(dA)−poly(dT) base pair domains, particularly the appearance of a sharp positive band at 260 nm in the longer dumbbells.[21] In addition, the sign and intensity of the long-wavelength CD bands (vide infra) are consistent with the separation of the PDI chromophores by a normal B-DNA base pair domain.

The UV absorption spectra of **D13** (Figure 1) and other dumbbells possessing nine or more A-T base pairs display a vibronic band progression in which the A^{0-0}/A^{0-1} band intensity ratio is 1.5(±0.1):1, characteristic of the PDI monomer.[16,24] The somewhat lower A^{0-0}/A^{0-1} band intensity ratio for the shorter dumbbells (Table 1) is attributed to equilibrium formation of aggregates having intermolecular PDI stacking. Increased aggregation for the shorter dumbbells is in turn attributed to decreased solubility in water, a consequence of the lower ratio of negatively charged phosphates to hydrophobic PDI linkers in the shorter dumbbell. As is the case for the formation of hairpin dimers from **H8**,[16] the band intensity ratios for all of the dumbbells decrease with increasing NaCl concentration. The formation and characterization of dumbbell aggregates in the presence of added salt will be described in greater detail elsewhere.

The fluorescence spectrum of **D8** in buffer (Figure 3) has a mirror image relationship to the absorption and fluorescence excitation spectra and displays a vibronic structure characteristic of the PDI monomer.[16] The fluorescence quantum yield ($\Phi_{fl} = 0.9 \times 10^{-2}$) is ca. 100-fold lower than that for a nonconjugated PDI monomer in organic solvents ($\Phi_{fl} \sim 1.0$).[24] The low fluorescence quantum yield is attributed to quenching of singlet

TABLE 2: Calculated Dumbbell Structural Parameters for D6, D8, and D13, and Calculated and Observed ECCD Intensities Relative to D6

conjugate	R_{ij}, Å	θ	sin(2θ)	R_{ij}^{-2} sin(2θ) calcd[a]	$\Delta\varepsilon_{obsvd}$[a]
D6	24.2	239	+0.88	+1.0	+1.0
D8	30.8	309	−0.98	−0.68	−0.58
D13	47.6	483	−0.92	−0.27	−0.14

[a] Normalized values relative to **D6**.

PDI by adjacent A-T base pairs, as previously reported for hairpin **H8**.[16]

Exciton Coupled Circular Dichroism. Further information pertaining to the dumbbell monomer structures is provided by the long-wavelength region of their CD spectra (Figure 4a). The CD spectrum of a monomer dumbbell is expected to display contributions from both the induced CD (ICD) of the individual PDI chromophores and the intramolecular exciton-coupled CD (EC-CD) of the two PDI chromophores. The spectrum of the monomer hairpin **H8** shown in the inset in Figure 4a provides a model for the PDI dumbbell ICD. The long-wavelength region of the CD spectra of **H8** in buffer displays a vibronic progression similar to that for the long-wavelength absorption band of monomeric PDI (Figure 1).[16] The negative sign is characteristic of the ICD of capping or intercalated chromophores whose transition dipoles are aligned approximately parallel to the long axis of the adjacent base pair(s).[25] Corrected EC-CD spectra for the dumbbells **D6**, **D8**, and **D13** obtained by subtraction of the ICD spectrum for **H8** from the observed spectra are shown in Figure 4b.[26]

The intensity of the long-wavelength EC-CD band for DNA capped hairpin or dumbbell structures in which the two chromophores are parallel and both are perpendicular to the DNA helical axis can be described by eq 1,

$$\Delta\varepsilon \approx \pm\frac{\pi}{4\lambda}\mu_i^2\mu_j^2 R_{ij}^{-2}\sin(2\theta) \qquad (1)$$

where λ is the wavelength of the transition, $\mu_{i,j}$ are the electronic transition dipole moments, R_{ij} is the distance vector, and θ is the angle between the PDI transition dipole moments.[6] Good agreement between the normalized calculated and observed CD intensities of the long-wavelength band is obtained using the calculated values of R_{ij} and an average helical pitch of 35°, somewhat larger than the calculated value of $\theta = 31 \pm 1°$ but closer to the value of 36° for B-DNA (Table 2).

The change in sign from positive for **D6** to negative for **D8** is similar to that previously reported for stilbenedicarboxamide-linked nicked dumbbells possessing the same number of A-T base pairs.[7] The intensities are ca. 25% larger for the PDI-linked versus stilbene-linked dumbbells, and the intensity for **D13** is comparable to that for a stilbenedicarboxamide capped hairpin possessing 11 base pairs.[7] The larger EC-CD intensity for PDI versus stilbene is consistent with its larger transition dipole moment for PDI versus stilbene ($\mu_{i,j} = 8.9$[27] versus 6.7 D[7]), which is partially mitigated by the longer wavelength of its optical transitions (eq 1). The observation of weak EC-CD for **D13** extends the usable range of the DNA "helical ruler" to nearly 50 Å. EC-CD has been observed over even longer distances using porphyrin chromophores attached to rigid molecules and helical polymers.[28] The PDI chromophore offers the advantage of longer wavelength absorption than either stilbene or the porphyrin Soret band.

SCHEME 2: Three-State Model for Base Pair Dissociation and PDI-PDI Association of Dumbbell D8

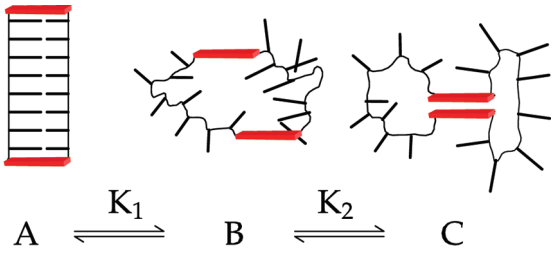

Thermal Dissociation of the Monomer Dumbbells. The thermal dissociation profiles obtained from the 260 nm absorption intensities and A^{0-0}/A^{0-1} band intensity ratios have complementary shapes and similar melting temperatures, indicative of the conversion of the base paired monomer dumbbell to a collapsed dumbbell having intramolecular PDI−PDI association. This conclusion is consistent with the minimized base-paired and melted structures for **D8** shown in Figure 5. Since intramolecular PDI association requires essentially complete base pair melting, it is reasonable to assume that intermediates having dissociated base pairs are formed prior to PDI association. The resulting three-state model is shown in Scheme 2. According to this scheme, the 260 nm thermal dissociation profile is determined by the coupled equilibria between the based-paired dumbbell A and the unpaired species B and C, whereas the A^{0-0}/A^{0-1} band intensity ratio is determined by the coupled equilibrium between the PDI−PDI stacked species C and the unstacked species A and B. The similar values of T_{260} and T_{ratio} for each of the dumbbells suggests that the free energies of B and C are similar. However, fitting of the two thermal dissociation profiles for the longer dumbbells provides different values of $\Delta H°$ and $\Delta S°$, apparently requiring the accumulation of B. These fits are not considered to be reliable, as a consequence of insufficient high temperature data (Figure 2b).

A method for determining the approximate concentration of B is provided by analysis of the UV spectral data, assuming that the mole fraction of A (χ_A) decreases from 1.0 to 0 over the temperature range 30−95 °C and that the mole fraction of C (χ_C)increases from 0 when $A^{0-0}/A^{0-1} = 1.5$ to 1.0 when $A^{0-0}/A^{0-1} = 0.6$, using the values for the monomer and dimer of hairpin **H8**.[16] The mole fraction of B (χ_B) can then simply be determined by subtraction ($\chi_B = 1 - [\chi_A + \chi_C]$). Plots of the calculated mole fractions versus temperature for **D16** and for **D13** and **D10** are shown in Figure 6 and Supporting Information Figure S5, respectively. The ratios χ_C/χ_B at high temperatures (75−95 °C) are ca. 3.7:1, 5:1, and >20:1 for **D16**, **D13**, and **D10**, respectively. Thus, a three-state model is necessary to account for the temperature dependent spectral data for the longest dumbbells **D16** and **D13**, whereas a two-state model which neglects species B provides an adequate description of the melting of the shorter dumbbells, in accord with the results of molecular dynamics simulations for **D8** (Figure 5).

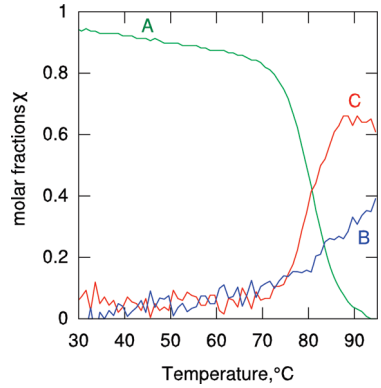

Figure 6. Temperature dependence of the mole fractions of species A, B, and C (Scheme 2) for **D16**.

The decrease in the ratio χ_C/χ_B with increasing base pair number at temperatures above T_{260} is consistent with the anticipated effect of temperature upon the equilibrium constant K_2 in Scheme 2. Increasing the length of the base pair domain should decrease the rate constant for PDI−PDI association but have little effect on the rate constant for PDI−PDI dissociation. Whereas the free energy changes associated with K_1 and K_2 cannot be determined reliably from the spectroscopic data, the relative enthalpies of the three species are expected to follow the order A ≪ C < B while the entropies are expected to follow the order B > C > A. Thus, all of the dumbbells exist predominantly as the base-paired species A at room temperature and B will become the predominant species only at temperatures significantly above the boiling point of water.

It is interesting to compare the dependence of the melting temperatures upon the length of the base pair domain (T_{260}, Table 1) for the PDI-linked dumbbells (T_{260}, Table 1) with those for related systems. We have reported that dumbbells having 6, 8, or 10 A-T base pairs connected by flexible hexa(ethylene glycol) PEG linkers all have relatively high T_{260} values (74, 76, and 78 °C, respectively).[2] Similarly, nicked hairpins having 6, 8, or 11 base pairs connected by stilbenedicarboxamide linkers all have high T_{260} values (72, 73, and 71 °C, respectively).[7] Analysis of the published 260 nm thermal dissociation profiles for the PEG-linked dumbbells using Meltwin[20] provides values of $-\Delta H° = 5.8 \pm 0.1$ kcal/mol per base pair and $-\Delta S° = 16.4 \pm 0.5$ cal/(mol K), indicative of nearly perfect entropy−enthalpy compensation in the PEG-linked dumbbells.[29] The significantly lower T_{260} values for the shorter PDI-linked dumbbells suggest that PDI−PDI association may compensate in part for the unfavorable enthalpy of base pair melting, with this compensation being the largest for the shortest dumbbells.

Concluding Remarks. Perylenediimide-linked synthetic dumbbells have been prepared by modification of the chemical ligation strategy used for the preparation of the analogous stilbenedicarboxamide-linked dumbbells.[5] These dumbbells exist predominantly as monomers in dilute aqueous buffer in the absence of added sodium chloride, as previously observed for PDI-linked hairpins.[16] The room temperature UV and fluorescence spectra (Figures 1 and 3) display vibronic band intensities characteristic of isolated PDI chromophores. The CD spectra are more complex, but they can be analyzed as a composite of the induced CD spectra of the monomer and the exciton-coupled CD spectra of the PDI chromophores on opposite ends of the dumbbell. The corrected EC-CD spectra (Figure 4b) are consistent with the vector model developed for the analysis of the EC-CD spectra of stilbenedicarboxamide capped hairpins,[7] extending the distance over which exciton coupling can be observed from 11 to 13 base pairs.

Upon heating, the PDI UV vibronic band intensities change and more nearly resemble those of the PDI−PDI dimer at high temperature (Figure 1). These changes are attributed to concomitant base pair dissociation and intramolecular PDI−PDI association, in accord with the results of molecular dynamics simulation of the melted duplex in water (Figure 5). Analysis of the thermal dissociation profiles for base-pair melting and PDI−PDI association using the three-state model shown in Scheme 2 provides approximate values for the mole fractions

of the three species having intact base pairs (A) and dissociated base pairs without PDI−PDI stacking (B) and with PDI−PDI stacking (C). The mole fraction of the intermediate species B is small for the shorter dumbbells, but it increases for the two longest dumbbells. The low melting temperatures of the shorter dumbbells are attributed to the partial compensation of PDI−PDI association for base pair dissociation.

Experimental Section

Synthesis of PDI Containing DNA Dumbbells. The mono-protected precursor of PDI linker **L** (Chart 1) was prepared by the method of Rahe et al.[17] The dumbbell precursors **P6−P13** (Scheme 1) were synthesized on a 3′-phosphate solid support following the procedure of Letsinger and Wu for the synthesis of bis(oligonucleotide) conjugates,[18] as modified by Rahe et al. for the incorporation of the PDI linker.[17] Solutions containing the nicked dumbbell precursors **P6−P13** were prepared in 250 mM MES buffer, pH 8.6 in the presence of 20 mM $MgCl_2$ and converted to **D6−D13** by the method of Carriero and Damha.[19] The solution was heated at 100 °C in a water bath for 10 min and then allowed to cool slowly to 4 °C. The annealed sample was further chilled in an ice bath for 15 min, and then 0.1 equiv volumes of 5 M CNBr in anhydrous acetonitrile were added. The reaction was quenched by addition of 1 equiv volume of 0.2 M TEAA followed by loading the mixture in a column packed with C18 resins. Excess reagents were removed by washing the column with 0.1 M TEAA, and the DNA products were eluted with 1:1 acetonitrile/0.1 M TEAA followed by 1:1 MeOH/H_2O. The collected products were evaporated to dryness and purified by HPLC to afford the ligated DNA dumbbell. The HPLC trace for the conversion of **P8** to **D8** is shown in Figure S1 in the Supporting Information. The yield of chemical ligation was 78%. The dumbbells have shorter retention times than their precursors and thus can be readily purified using RP-HPLC. Since one water molecule is lost during the ligation reaction, the resulting dumbbells possess molecular weights that are 18.03 Da less than their corresponding precursors. Therefore, the identities of the dumbbell structures can be verified using MALDI-TOF ms (Table S1, Supporting Information). The yields of the ligated dumbbells are dependent upon the length of the A-tract sequences, increasing from 70% for **D6** to >95% for **D16**.

Methods. Procedures used for the recording of UV−visible, fluorescence, and circular dichroism spectra have been described.[16]

Acknowledgment. This research is supported by a grant from the National Science Foundation, Collaborative Research in Chemistry for the project DNA Photonics (CHE-0628130 to G.C.S. and F.D.L.).

Supporting Information Available: MALDI data, typical HPLC trace, temperature dependent UV, fluorescence, and CD spectra, and calculated mole fractions. This material is available free of charge via the Internet at http://pubs.acs.org.

References and Notes

(1) Doktycz, M. J.; Paner, T. M.; Benight, A. S. *Biopolymers* **1993**, *33*, 1765–1777.

(2) McCullagh, M.; Zhang, L.; Karaba, A. H.; Zhu, H.; Schatz, G. C.; Lewis, F. D. *J. Phys. Chem. B* **2008**, *112*, 11415–11421.

(3) Herrlein, M. K.; Nelson, J. S.; Letsinger, R. L. *J. Am. Chem. Soc.* **1995**, *117*, 10151–10152.

(4) Herrlein, M. K.; Letsinger, R. L. *Angew. Chem., Int. Ed.* **1997**, *36*, 599–601.

(5) Zhang, L.; Long, H.; Schatz, G. C.; Lewis, F. D. *Org. Biomol. Chem.* **2007**, *5*, 450–456.

(6) Lewis, F. D.; Liu, X. Y.; Wu, Y. S.; Zuo, X. B. *J. Am. Chem. Soc.* **2003**, *125*, 12729–12731.

(7) Lewis, F. D.; Zhang, L.; Liu, X.; Zuo, X.; Tiede, D. M.; Long, H.; Schatz, G. C. *J. Am. Chem. Soc.* **2005**, *127*, 14445–14453.

(8) Lewis, F. D.; Zhang, L. G.; Zuo, X. B. *J. Am. Chem. Soc.* **2005**, *127*, 10002–10003.

(9) Lewis, F. D. *Photochem. Photobiol.* **2005**, *81*, 65–72.

(10) (a) Förster, T. *Ann. Phys.* **1948**, *2*, 55–75. (b) Lakowicz, J. R. *Principles of Fluorescence Spectroscopy*, 2nd ed.; Kluwer Academic: New York, 1999.

(11) (a) Wang, W.; Wan, W.; Zhou, H. H.; Niu, S. Q.; Li, A. D. Q. *J. Am. Chem. Soc.* **2003**, *125*, 5248–5249. (b) Che, Y.; Yang, X. M.; Zang, L. *Chem. Commun.* **2008**, 1413–1415.

(12) (a) Abdalla, M. A.; Bayer, J.; Radler, J. O.; Müllen, K. *Angew. Chem., Int. Ed.* **2004**, *43*, 3967–3970. (b) Bayer, J.; Radler, J. O.; Blossey, R. *Nano Lett.* **2005**, *5*, 497–501.

(13) Zheng, Y.; Long, H.; Schatz, G. C.; Lewis, F. D. *Chem. Commun.* **2005**, 4795–4797.

(14) Ustinov, A. V.; Dubnyakova, V. V.; Korshun, V. A. *Tetrahedron* **2008**, *64*, 1467–1473.

(15) (a) Bevers, S.; O'Dea, T. P.; McLaughlin, L. W. *J. Am. Chem. Soc.* **1998**, *120*, 11004–11005. (b) Bevers, S.; Schutte, S.; McLaughlin, L. W. *J. Am. Chem. Soc.* **2000**, *122*, 5905–5915. (c) Zheng, Y.; Long, H.; Schatz, G. C.; Lewis, F. D. *Chem. Commun.* **2006**, 3830–3832.

(16) Hariharan, M.; Zheng, Y.; Long, H.; Zeidan, T. A.; Schatz, G. C.; Vura-Weis, J.; Wasielewski, M. R.; Zuo, X. B.; Tiede, D. M.; Lewis, F. D. *J. Am. Chem. Soc.* **2009**, *131*, 5920–5929.

(17) Rahe, M.; Rinn, C.; Carell, T. *Chem. Commun.* **2003**, 2120–2121.

(18) Letsinger, R. L.; Wu, T. *J. Am. Chem. Soc.* **1995**, *117*, 7323–7328.

(19) Carriero, S.; Damha, M. J. *Org. Lett.* **2003**, *5*, 273–276.

(20) McDowell, J. A. *MeltWin 3.5*; 2001.

(21) Johnson, W. C. In *Circular Dichroism, Principles and Applications*; Berova, N., Nakanishi, K., Woody, R. W., Eds.; Wiley-VCH: New York, 2000; p 703−718.

(22) Berova, N.; Nakanishi, K. In *Circular Dichroism*; Berova, N., Nakanishi, K., Woody, R. W., Eds.; Wiley-VCH: New York, 2000.

(23) Bloomfield, V. A.; Crothers, D. M.; Tinoco, I., Jr. *Nucleic Acids, Structures, Properties, Functions*; University Science Books: Sausalito, CA, 2000.

(24) Giaimo, J. A.; Lockard, J. V.; Sinks, L. E.; Scott, A. M.; Wilson, T. M.; Wasielewski, M. R. *J. Phys. Chem. A* **2008**, *112*, 2322–2330.

(25) Ardhammar, M.; Kurucsev, T.; Nordén, B. In *Circular Dichroism, Principles and Applications*; Berova, N., Nakanishi, K., Woody, R. W., Eds.; Wiley-VCH: New York, 2000; p 741−768.

(26) The presence of an equilibrium between monomer and aggregate is not expected to alter the observed or corrrected CD spectra of **D6**, as the hairpin dimer of **H8** has a very weak CD spectrum.

(27) Sadrai, M.; Hadel, L.; Sauers, R. R.; Husain, S.; Krogh-Jespersen, K.; Westbrook, J. D.; Bird, G. R. *J. Phys. Chem.* **1992**, *96*, 7988–7996.

(28) (a) Matile, S.; Berova, N.; Nakanishi, K.; Fleischhauer, J.; Woody, R. W. *J. Am. Chem. Soc.* **1996**, *118*, 5198–5206. (b) Tsubaki, K.; Takaishi, K.; Tanaka, H.; Miura, M.; Kawabata, T. *Org. Lett.* **2006**, *8*, 2587–2590.

(29) (a) Searle, M. S.; Williams, D. H. *Nucleic Acids Res.* **1993**, *21*, 2051–2056. (b) Petruska, J.; Goodman, M. F. *J. Biol. Chem.* **1995**, *270*, 746–750.

JP1048309